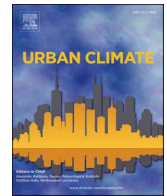




ELSEVIER

Contents lists available at [ScienceDirect](https://www.sciencedirect.com)

Urban Climate

journal homepage: www.elsevier.com/locate/uclim

How local climate zones influence urban air temperature: Measurements by bicycle in Dijon, France

Justin Emery^{a,*}, Benjamin Pohl^b, Julien Crétat^b, Yves Richard^b, Julien Pergaud^b, Mario Rega^b, Sébastien Zito^b, Julita Dudek^b, Thibaut Vairet^{b,c}, Daniel Joly^c, Thomas Thévenin^c

^a Université de technologie de Compiègne, AVENUES, Centre Pierre Guillaumat - CS 60 319 - 60 203, Compiègne Cedex, France

^b Centre de Recherches de Climatologie, UMR 6282 Biogéosciences, CNRS/Univ Bourgogne Franche-Comté, France

^c UMR 6049 THEMA, CNRS/Univ Bourgogne Franche-Comté, France

ARTICLE INFO

Keywords:

UHI
Urban form
LCZ
Iterated transect
ANalysis of VAriance
Thermal impacts

ABSTRACT

This study analyses mobile measurements of urban temperatures in Dijon (eastern France) to quantify the influence of urban form on the micro-scale variability of air temperature. A route was ridden identically on 33 spring and summer evenings on a bike fitted out with measuring instruments (VeloClim). These evenings followed sunny calm days conducive to the formation of thermal contrasts and urban heat islands (UHIs). Two typologies, Corine Land Cover (CLC) and Local Climate Zones (LCZ), are used to assess the impact of urban form and land cover on air temperatures based on ANalysis Of VAriance (ANOVA). ANOVA is applied to the mean of runs to maximize the effect of surface states, and to each run individually to maximize the influence of weather conditions.

The results show that both typologies prove relevant and complementary for studying the impact of vegetated and artificialized zones on urban temperature. Temperature variations on intra-urban scales are significantly modulated by urban form and land cover types. Vegetated areas are systematically cooler than impervious surfaces. Independently of meteorological conditions, urban form has a decisive influence on air temperature and each CLC or LCZ category has an original air temperature signature.

1. Introduction

Urban heat islands (UHIs) have been studied for over 100 years now (Stewart, 2019). They are defined in terms of the variation between background rural temperatures and peak urban temperatures (Oke, 1973). Pioneering works from the early nineteenth to the early twentieth century highlighted the impact of cities on temperatures (Howard, 1833; Renou, 1868). Innovative methodology from 1920 to 1940 contributed to quantifying and mapping this effect (Schmidt, 1927) and experimental studies from 1950 to 1980 provided a better understanding of it (Sundborg, 1951). The present study stems from work done on innovative methods for measuring urban temperature by means of a mobile campaign. It assesses the influence of land surface properties on temperature in an urban environment and the associated uncertainties induced by the approximation of surface properties.

Urban characteristics and the diversity of materials in built-up areas may contribute to the warming of the urban boundary layer

* Corresponding author.

E-mail address: justin.emery@utc.fr (J. Emery).

<https://doi.org/10.1016/j.uclim.2021.101017>

Received 27 January 2021; Received in revised form 5 October 2021; Accepted 25 October 2021

2212-0955/© 2021 Elsevier B.V. All rights reserved.

(Oke, 1973), including surface temperatures (Berg and Metzler, 1934; Takahashi, 1959; Unger et al., 2010), and to the intensification of UHIs (Runnalls and Oke, 2013). By contrast, vegetated areas tend to lower surface temperatures, both locally and within a radius 300–1000 m (Petralli et al., 2014), and promote urban cool islands (UCIs). UHIs are both more intense and more frequent in the evening and throughout the night (Berg and Metzler, 1934; Eliasson, 1996; Runnalls and Oke, 2013) because paved surfaces slow and reduce night time cooling, whereas cooling occurs more rapidly in vegetated areas (Berg and Metzler, 1934; Sun et al., 2009; Sun, 2011; Heusinkveld et al., 2014; Song et al., 2014). UHIs contribute to increased thermal stress and even mortality among the urban population, as has been reported in France (Fouillet et al., 2006; Pascal et al., 2018) and Europe (Robine et al., 2008). The increasing

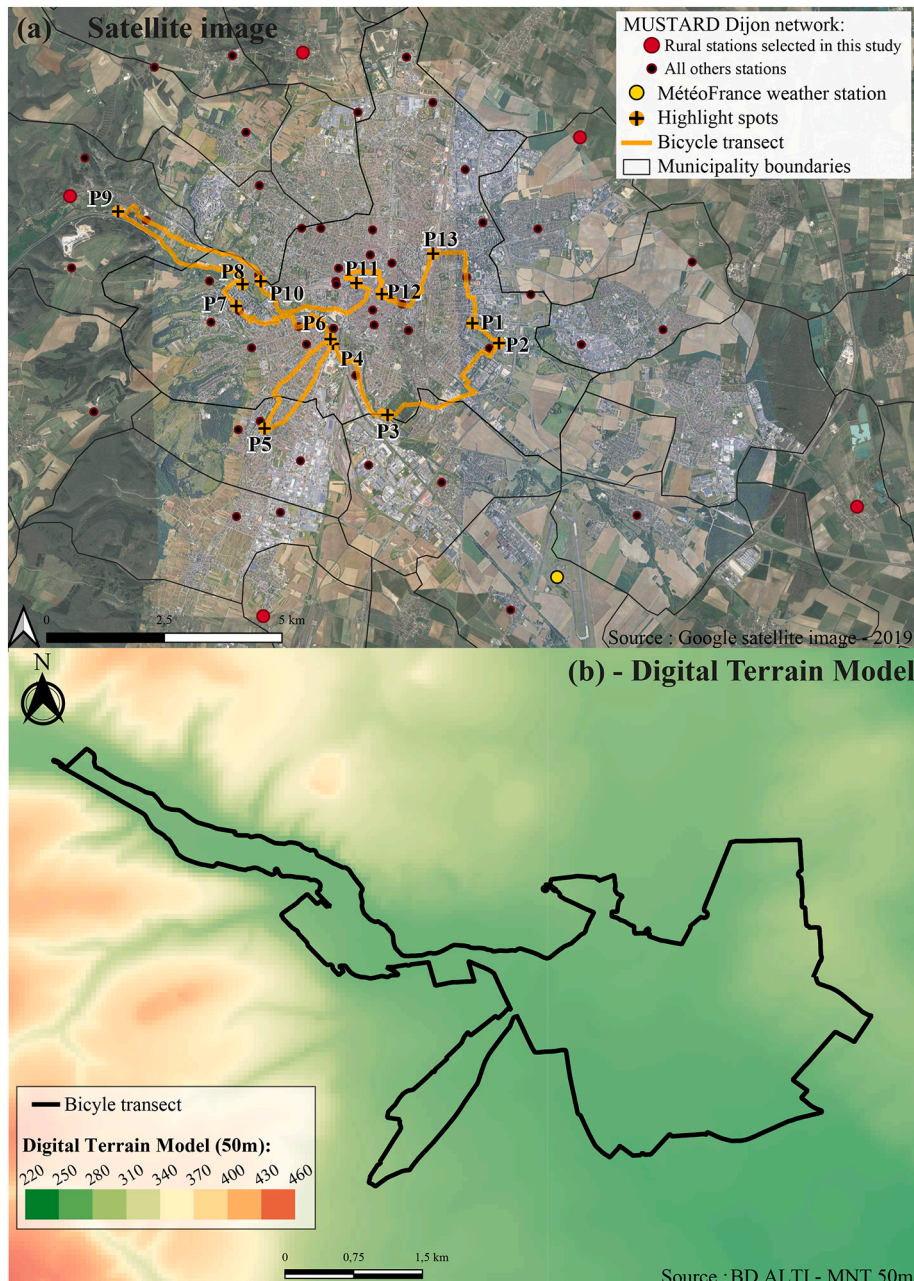


Fig. 1. Spatial characteristics of the mobile measurements. (a) Transect of the mobile measurement of temperature in Dijon Métropole and location of the MUSTARDijon network recording hourly temperatures. The rural stations in red are used to produce thermal indicators. The Météo-France weather station in yellow is used to characterize the general weather conditions of the runs. P1 to P13 are the highlight spots along the transect used to divide the transect in smaller units homogeneous in terms of surfaces properties (downtown, urban parks, dense built-up areas...). (b) Digital Terrain Model at 50-m resolution. (For interpretation of the references to colour in this figure legend, the reader is referred to the web version of this article.)

frequency, duration and intensity of heatwaves further amplify their adverse effects on health (Hajat et al., 2010; Tan et al., 2010; Revi et al., 2014). An understanding of the dynamics of the urban climate and the impacts of urban properties on temperatures may pave the way for sustainable urbanization with the potential to improve thermal comfort and reduce mortality in urban areas (Revi et al., 2014). Improving cities' resilience with respect to climate hazards is an issue of increasing importance that needs to be achieved through low-carbon strategies.

Achieving this requires a capacity to characterize properties in urban areas and temperature fluctuations in time and space. Many modern typologies have been developed to characterize the properties of cities worldwide (see Lehnert et al., 2021 for a review) and to assess the impact of urban form and land cover on urban climate. Among them, two complementary typologies, widely used across Europe, have proved to be suitable for urban climate studies (Zhou et al., 2013; Leconte et al., 2015; Petrișor and Petrișor, 2015; Lehnert et al., 2018; Richard et al., 2018): Corine Land Cover (CLC; Büttner et al., 2002) and Local Climate Zone (LCZ; Stewart and Oke, 2012). The CLC typology provides a macro-scale view of urban areas (Zhou et al., 2013; Petrișor and Petrișor, 2015) with potentially relevant information for climate (and climate modelling), such as the density of impervious surfaces or of vegetation types. The LCZ typology is a climate-related approach designed for studying UHIs and facilitating comparison across cities regardless of their size, geographical location, urban structure, building characteristics and land-cover types (Stewart and Oke, 2012). The LCZ typology provides a local-scale summary of urban areas accounting for both surface properties (building heights and densities) and land cover (permeability, vegetation). Therefore the two typologies allow us to characterize the urban form, defined as the spatial relation between physical features, natural physical forms and built physical forms (Kropf, 2009, 2014), on two complementary scales.

As a result of increased experimentation and methodological innovation to describe the heat island phenomenon (Stewart, 2019), several methods have been developed for measuring urban air temperature. The most widely used are networks of fixed stations generally spaced a few hundred meters to a few kilometres apart. A network density of this order yields information on a local scale ranging from 10^2 to 5×10^4 m (Oke, 1987). Such networks have the advantage of regular repeatability (hourly or even sub-hourly measurements).

In Dijon Métropole (Burgundy, France), the Measuring Urban System of Temperature of Air Round Dijon (MUSTARDijon) was first introduced in 2014 to monitor air temperature (Richard et al., 2018, 2021). With 47 stations (Fig. 1), this network has demonstrated the relevance of the CLC and LCZ typologies for characterizing coherent thermal environments (Richard et al., 2018) and studying UHI intensity during hot spells and heat waves (Richard et al., 2021).

Nevertheless, the MUSTARDijon network was not designed to measure temperature variations on the micro-scale which is the most relevant scale for urban planning (Ng et al., 2015). On such micro-scales, 10^2 to 10^3 m (Renou, 1868; Hann, 1885; Oke, 1987; Buttstädt et al., 2011; Tsin et al., 2016), mobile measurements are more appropriate (Tsin et al., 2016) since they sample temperature at high frequencies within and between urban form categories (Brandsma and Wolters, 2012; Buttstädt et al., 2011; Lehnert et al., 2018). Since they were first used in Europe in the 1920s, mobile measurements have been widely employed to assess the impact of urban form on intra-urban temperature patterns (see the review by Stewart, 2019). Mobile measurements, whether made on foot (Brooks, 1931; Tsin et al., 2016), by bicycle (Budel and Wolf, 1933; Brandsma and Wolters, 2012; Heusinkveld et al., 2014; Rajkovich and Larsen, 2016; Lehnert et al., 2018) or with motorized vehicles (Schmidt, 1927; Peppler, 1929; Fukui and Wada, 1941; Hart and Sailor, 2009; Buttstädt et al., 2011; Sun et al., 2009; Sun, 2011; Leconte et al., 2017), have the drawback of coarse and often irregular sampling over long time-period.

By combining urban form data, fixed networks and mobile measurements, it becomes possible to observe the spatio-temporal variability of air temperature driven by surface properties on local and micro scales (Buttstädt et al., 2011; Fenner et al., 2014; Leconte et al., 2017; Beck et al., 2018; Lehnert et al., 2018). For instance, Fenner et al. (2014) show that temperatures recorded at fixed stations in Berlin (Germany) are modified by the different LCZs and their distinct surface properties. Similar findings have been obtained using mobile measurements in Olomouc (Czech Republic) (Lehnert et al., 2018). Night time air temperatures recorded in Nancy (France) reveal frequent UHIs with temperature differences of 0.5°C to 2°C in urbanized LCZ categories compared to natural categories (Leconte et al., 2017). All these studies use LCZs to describe and help relate UHIs to urban characteristics.

Most of the above mentioned studies address the impact of urban form on temperature variability on local to micro scales (a few metres). However, it is still unclear to what extent such impacts may be sensitive to the choice of the urban form typologies. This study aims to fill this gap by examining the influence of CLC and LCZ typologies on the local to micro scale variability of temperature. To that end, we conducted a campaign of mobile temperature measurements along an iterated transect accounting for the diversity of surface properties in Dijon Métropole.

The paper is organized as follows. Section 2 presents the Dijon Métropole urban area, the mobile measurements and CLC/LCZ typologies, as well as the method used to assess their impact on temperature. Section 3 presents and validates the LCZ categories in Dijon Métropole and assesses the impact of the two typologies on the spatio-temporal variability. Sections 4 and 5 present the discussion and the main conclusions, respectively.

2. Study area, material and method

2.1. The Dijon Métropole urban area

The study was conducted in Dijon Métropole in Burgundy, eastern France. This conurbation extends over ~ 240 km² in a radio-concentric pattern (Fig. 1a). It covers 23 boroughs (*communes*) and with its 260,000 or so inhabitants is typical of mid-size cities in Western Europe (Giffinger et al., 2010; Giffinger et al., 2007). The elevation of the conurbation varies from 220 m to 460 m westward (Fig. 1b). Its western part is marked by a plateau incised by a steep-sided valley where forest dominates. Its eastern part is marked by a

plain with openfield type cereal farmland. Dijon Métropole is characterized by warm/cold temperatures and dry/wet conditions during summer/winter (Kottek et al., 2006) and by marked/weak interannual variability in temperature/precipitation (Joly et al., 2010).

2.2. Corine land cover and local climate zone typologies

Two typologies are used to examine the potential impact of urban form (local surface structure, cover, fabric, and metabolism) on air temperature. The CLC typology (Büttner et al., 2002), produced in 2012, groups land-cover into 44 categories based on satellite images using a minimum mapping unit of 25 ha for raster data and a minimum width of 100 m for vectorial data. The CLC typology is efficient at identifying well-structured patterns of land cover (e.g. artificial, agricultural and humid areas) but does not allow for a detailed characterization of urban form at local scale (e.g. no distinction between buildings and roads, or between low- and high-rise buildings) (Petrişor and Petrişor, 2015).


To overcome this limitation, we also consider the LCZ typology developed by Stewart and Oke (2012). LCZs list urban and rural environments in 17 categories mixing local-scale criteria (e.g. building density and height, vegetation density and type). Of the different methods developed for mapping LCZs (Lehnert et al., 2021), we used the WUDAPT (World Urban Database and Access Portal Tools) method (Brousse et al., 2016; Ching et al., 2018), which effectively delineates LCZs (Verdonck et al., 2017) and produces results very similar to more sophisticated approaches such as Geographical Information System methods (Gál et al., 2015). The WUDAPT method maps LCZs based on semi-automatic classification algorithms applied to satellite images (Bechtel and Daneke, 2012; Brousse et al., 2016; Bechtel et al., 2019). Following Ching et al. (2018), this classification has been constructed from a set of training areas in Dijon Métropole based on high-resolution Google Earth images. Except for this critical point, the WUDAPT method is objective, simple and suitable for any city. We defined 70 training areas in Google Earth for the subsequent classification of multispectral Landsat-8 data available for seven dates in the SAGA-GIS software (23 September 2013, 11 April 2015, 19 July 2015, 14 August 2016, 30 August 2016, 2 January 2017 and 8 March 2017). Taking multiple Landsat-8 images at different times is important to capture the spectral response of vegetation due to seasonality (Bechtel and Daneke, 2012). The LCZ typology for Dijon Métropole (termed the level 0 product in WUDAPT) was generated at 100 m-resolution and is presented and compared to CLC in section 3.

2.3. Bicycle measurement protocol

2.3.1. Mobile meteorological station: VeloClim

The temperature data were collected using a cargo bike (called VeloClim: Fig. 2) equipped with a 2 m mast, and forming an effective, low-carbon way to measure urban climate (Brandtsma and Wolters, 2012; Heusinkveld et al., 2014; Rajkovich and Larsen, 2016; Lehnert et al., 2018). The instruments, their technical characteristics and positioning on VeloClim are shown in Fig. 2 and summarized as follows:

- Georeferencing of the transect every 5 m, using a differential GPS (1) connected to a GPS antenna (1) at the top of the mast;
- Temperature (2) and humidity (3) measurements every second via a HOBO U23 v2 sensor located in an M-RSA solar radiation shield (4) and attached to a data logger (5). According to HOBO, the temperature sensor has a response time of ~ 180 s at a speed of



	Instruments	Components	Data accuracy
1	GPS	Trimble GeoExplorer 2008 series	depends on the number of satellites and correction accuracy
2	Temperature sensor	HOBO Pro V2 U23-004	± 0.21 °C / ± 0.2 °C
3	Humidity sensor	Temperature/RH Smart Sensor : S-THB-M00X	$\pm 2.5\%$ between 10% and 90%
4	Solar radiation shield	M-RS3b	
5	Data logger	HOBO micro station	depends on the instrument
6	Anemometer	Wind Speed Smart Sensor : S-WDA-M003	± 1.1 m/s
7	Weather vane	Wind Direction Smart Sensor : S-WDA-M003	$\pm 5^\circ$

Fig. 2. Technical characteristics of the VeloClim measurement devices.

1 m.s⁻¹. In fact, sensitivity tests comparing fixed and mobile temperature measurements point to a response time of ~30 s at a speed of 5 m.s⁻¹, which corresponds to the mean speed of the VeloClim during the campaign. The 30 s lag has been accounted for by (i) taking a 30 s break before entering vegetated areas and (ii) applying a spatial filter to avoid mixed influences of different CLCs/LCZs on temperature, thereby eliminating a sizeable part of the problem by disregarding temperatures 200 m upstream and downstream of each CLC/LCZ (see section 3.2.2);

- Wind measurement taken only when the bike is at rest, at 13 locations along the transect, using an anemometer (6) and a wind vane (7) mounted on either side of the mast (not analysed in this study).

2.3.2. Bicycle transect: An iterated measurement protocol

A campaign of 33 mobile measurement runs was conducted from 2016 to 2018. All 33 runs were carried out in late spring or summer (April to August) from late afternoon to early night (19 to 22 UTC) to maximize city-countryside thermal contrasts (Richard et al., 2018). The runs all followed the same relatively flat (i.e. 40 m difference between the lowest and highest points) transect of 33.9 km (Fig. 1b). The transect was ridden in about 2 h 30 min with VeloClim and air temperature was recorded every 5 m, 2 m above the ground level. The transect was designed to be representative of the urban area by crossing over various types of surfaces and spaces ranging from dense zones like the city centre to vegetated zones, mostly in the outskirts. The transect and the different LCZs crossed along the transect are detailed in section 3.

Fig. 3 shows the weather conditions during and a few days prior to each run, as provided by the Météo-France synoptic weather station located south of Dijon (yellow dot in Fig. 1a). All runs were associated with pleasant calm weather conditions conducive to the formation of heat contrasts, that is high temperature, little wind, few clouds in the daytime before and rather dry conditions at least during two days prior to the runs. During the hours when the runs were carried out, temperatures generally fluctuated between 22 and 26 °C, relative humidity levels between 50 and 65% and wind speeds between 1.5 and 3 m.s⁻¹ (Fig. 3a-c). During the entire day of the runs, the weather was systematically very sunny (Fig. 3d) and without rain (Fig. 3e). Nevertheless, rain was sometimes observed during the previous days (Fig. 3e).

Nine out of the 33 runs were affected by instrument malfunctions or major gaps in GPS reception and are not analysed in this study. A few spatially-limited values were also missing in the 24 remaining runs due to GPS reception gaps. These missing values were replaced over the same transect by statistical interpolation (see section 2.3.3) assuming the VeloClim moved at constant speed (~5 m.s⁻¹) over the time when gaps occurred.

2.3.3. VeloClim data: Rural index and calibration of mobile measurements

Since not all runs were made at the same time of the same season and did not all last exactly 2 h 30 min, the raw temperature records were standardized in two stages to ensure the measurements are comparable. Furthermore, this allows us to compute synchronous temperature differences between rural background temperatures and urban mobile temperatures.

The first stage ensures synchronization over the same transect of data logged jointly by the differential GPS and the HOBO sensor. This processing corrects time discrepancies between the two devices and then uses the nearest neighbour method to project all observations onto a single standard transect of 6800 points. The second stage takes account of the time changes in temperature between departure and the end of the run. To that end, we use the MUSTARDijon network to compute temperature gradients between the city and countryside via observations recorded at five rural stations located at altitudes very close to those of the transect (cf. red dots in Fig. 1a). This adjustment takes account of the observation times between the mobile measurements and reference station

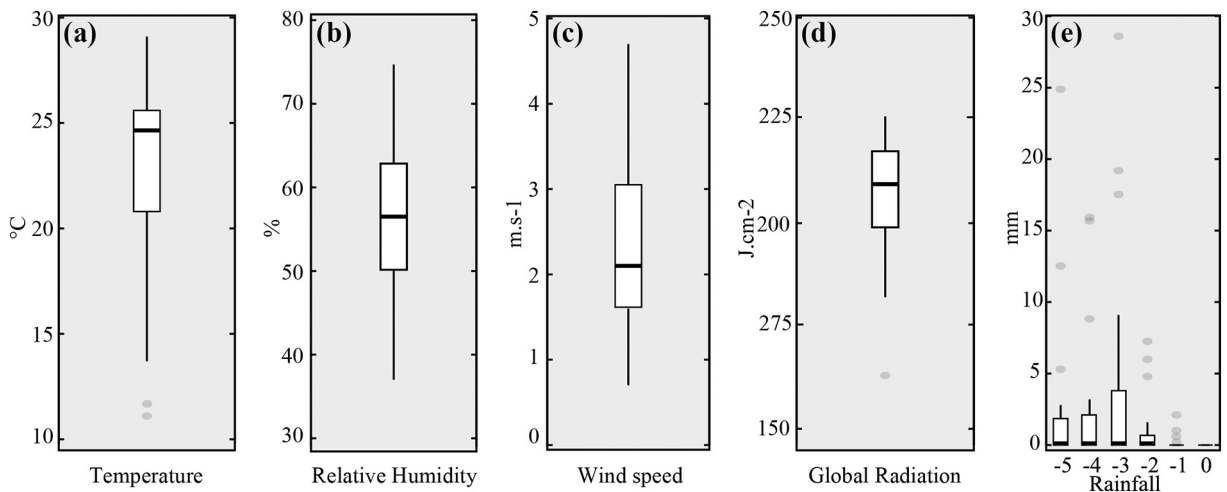


Fig. 3. Meteorological conditions at Dijon Longvic (Météo-France station) for the period of measurement. (a) Temperature at 2 m (19:00–21:00 UTC mean). (b) Relative humidity (19:00–21:00 UTC mean). (c) Wind speed at 10 m (19:00–21:00 UTC mean). (d) Global radiation (06:00–18:00 UTC mean). (e) Rainfall (daily accumulation) during the 5 days preceding the runs.

measurements (Brandsma and Wolters, 2012; Rajkovich and Larsen, 2016) to calculate the calibrated and validated temperature differences between mobile measurements in the city and fixed measurements in the rural area. These temperature differences are then used and analysed extensively in the remainder of this work.

2.4. Assessing the impact of CLCs and LCZs on temperature

The impact of CLCs or LCZs on air temperature is assessed in two stages. First, we qualitatively discuss the mean impact of urban form on temperature by plotting the mean temperature profile (i.e., the temperature difference against the rural index averaged for the 24 runs) along the transect together with the different CLCs/LCZs along it. Second, we quantify the urban form impact on temperature for each of the 24 runs through analyses of variance (ANOVAs: von Storch and Zwiers, 1999). ANOVAs are used to decompose total temperature variance according to the CLC or LCZ typology and to test whether temperature contrasts occur mostly between the categories of each typology, or within them. In ANOVAs, the total sum of squares (SST, the squared terms being deviations of each

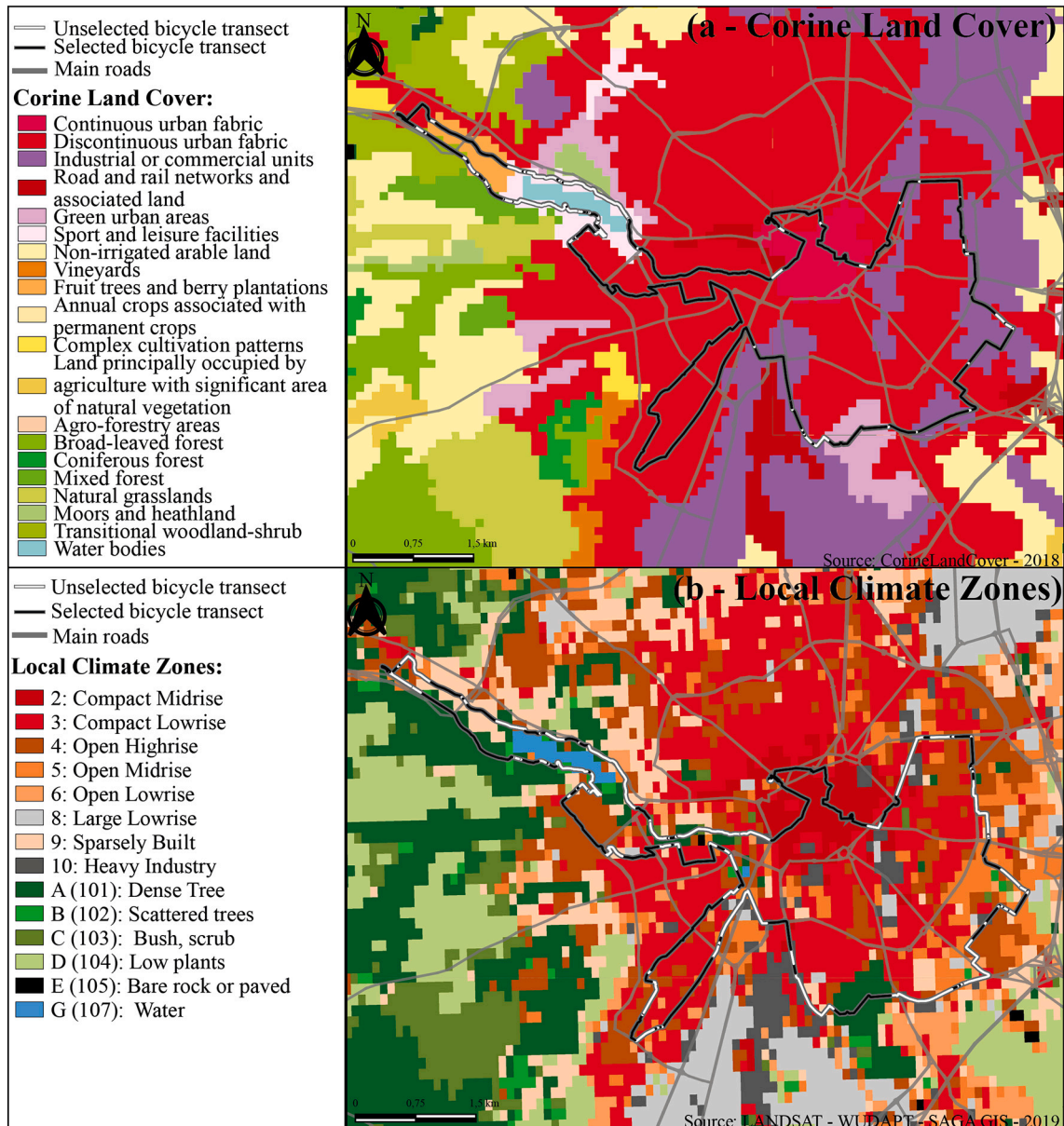


Fig. 4. Classification of Dijon Métropole surface properties. (a) Corine Land Cover (version 2012 - Büttner et al., 2002). (b) Local Climate Zones - Level 0 (Stewart and Oke, 2012). The black and white line shows the bicycle transect. The black line represents the sample used for analysis. The white line represents transition zones between different CLCs/LCZs, which are not analysed in this study.

temperature reading from the mean temperature regardless of the CLC/LCZ typology) is used to express the total variation of temperature that can be attributed to the various categories (i.e. the N CLCs or M LCZs). SST is then decomposed into the CLC/LCZ typology as follows:

$$SST = SS_{LCZ1} + SS_{LCZ2} + SS_{LCZ3} + \dots + SS_{LCZG} \tag{1}$$

with SS , the squared deviations of each temperature record within a CLC/LCZ category from the mean temperature of the corresponding category.

The F -test is used for determining the significance of the decomposition. The null-hypothesis is that the CLC/LCZ typology does not impact temperature, i.e., the temperature variance between the different categories is significantly weaker than the temperature variance within each category. Since the F -test is sensitive to non-normal distributions, we verify the normality of temperature distributions both regardless of and according to the CLC/LCZ typology using the Shapiro-Wilk test (Shapiro and Wilk, 1965) at the 95% confidence level. Temperatures recorded for each of the 24 runs are found to comply with a normal distribution for 100% of the runs regardless of the CLCs/LCZs and for 60% of the runs when tests are applied to individual CLC/LCZ categories.

Following Lehnert et al. (2018) and Geletić and Lehnert (2016), we use the Tukey test, also called Honestly Significant Difference (Tukey, 1962; Haynes, 2013), to identify urban form categories associated with temperatures that significantly differ from those of a reference category. CLC 111 (continuous urban fabric) and LCZ 2 (compact midrise) are selected as the references for the CLC and LCZ typologies respectively, since they correspond to densely built and little vegetated areas of the city centre.

3. CLC and LCZ contributions to urban air temperature

3.1. Assessment of CLC and LCZ typologies

Fig. 4 shows the 20 CLCs and 14 LCZs, as defined in section 2.2, for Dijon Métropole. The CLC typology provides spatially smoothed categories of land-use, with a predominance of impervious surfaces within and around the city centre and permeable surfaces in the surrounding rural environment (Fig. 4a). The most frequently recurring categories are the discontinuous urban fabric (53%), industrial or commercial units (16%) and sport and leisure facilities (11%). This simple partitioning is much more detailed and subtler when viewed on the LCZ spectrum (Fig. 4b). The partitioning is more homogeneous among the LCZs, with e.g. 20% of the city classified as LCZ 3 and another 20% as LCZ 4.

In detail, the dense medieval city centre (LCZ 2) is surrounded by two rings of boulevards. The inner Haussman-type ring serves the city centre whereas the outer one serves dense residential areas (LCZ 3) and large collective infrastructures (LCZ 5: regional hospital, university campus, etc.). Although the city centre is dense and largely impervious, vegetation is not entirely absent and makes up nearly 4.3% of the area. The residential space (LCZs 3 and 4) is vegetated and less densely built than LCZ 2 (vegetation and buildings cover 8.9% and 15.4% of the area, respectively). The urban area is also less densely built around trading estates (LCZs 8 and 10) and lower-density residential areas (LCZs 5 and 6) out to the peri-urban boroughs (LCZ 9) of the conurbation. Other noticeable characteristics of the Dijon metropolitan area concern a 33 ha urban park with dense vegetation (LCZ A) located south of the city centre, as well as scattered vegetation (LCZs B and C) around water bodies.

More particularly, the LCZ categories crossed along the transect (Fig. 5) can be summarized as follows (see also Fig. 1a for the

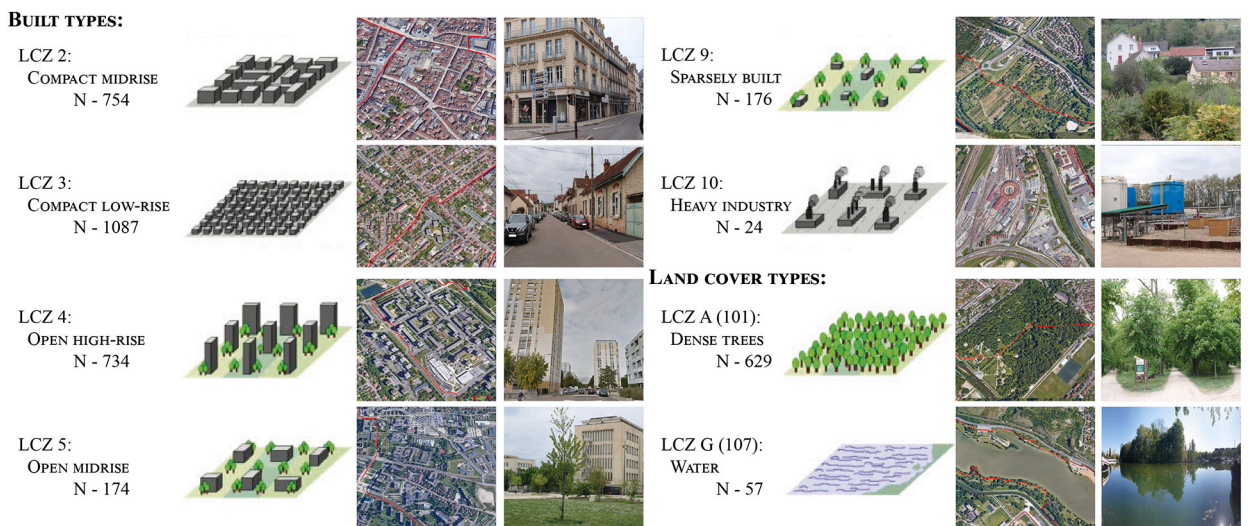


Fig. 5. Main LCZs along the VeloClim transect used to assess the impact of urban form on temperature. N corresponds to the number of classified pixels selected for the analysis. Copyright: Diagrams from Stewart and Oke (2012); Satellite images from CNES/Airbus, Maxar Technologies and Google Earth. All photographs by the authors except LCZ G by Claire Fabre.

location of highlight spots - P):

- (i) the eastern part of the transect (P1–P6) is in the lowland area (mean elevation 250 m) mostly in the urban space. At highlight spot P3, the route runs through a 33 ha park (LCZ A) before heading north through a trading estate (LCZs 8 and 10) and then a cycle/tow path (LCZs B and D). It runs south between P4 and P6 through a residential area (LCZs 3 and 4);
- (ii) the western part of the transect (P6–P11) leads around a man-made lake (LCZ G) in a steep-sided valley. This part runs through less densely built areas (LCZs 5 and 7) surrounded by forest (LCZ A), allotments (LCZ 6) in the far west, and then along the main river of the conurbation before coming back to the city centre (LCZ 2);
- (iii) the third section (P11–P13 then back to P1) runs through the medieval city centre and two small urban parks, after highlight spots P11 and P12, covering 2.5 ha and 0.4 ha, respectively. The route then ends by climbing a small hill (P13 towards P1) characterized by a more open urban space (LCZ 5) and vegetated space around large tertiary infrastructures (sports stadium, hospital grounds, and university campus) and the outer boulevards.

Impervious surfaces represent ~75% of the surface crossed along the transect regardless of the typology. Except for LCZ G, the route passes directly through the main LCZs, as illustrated in Fig. 5.

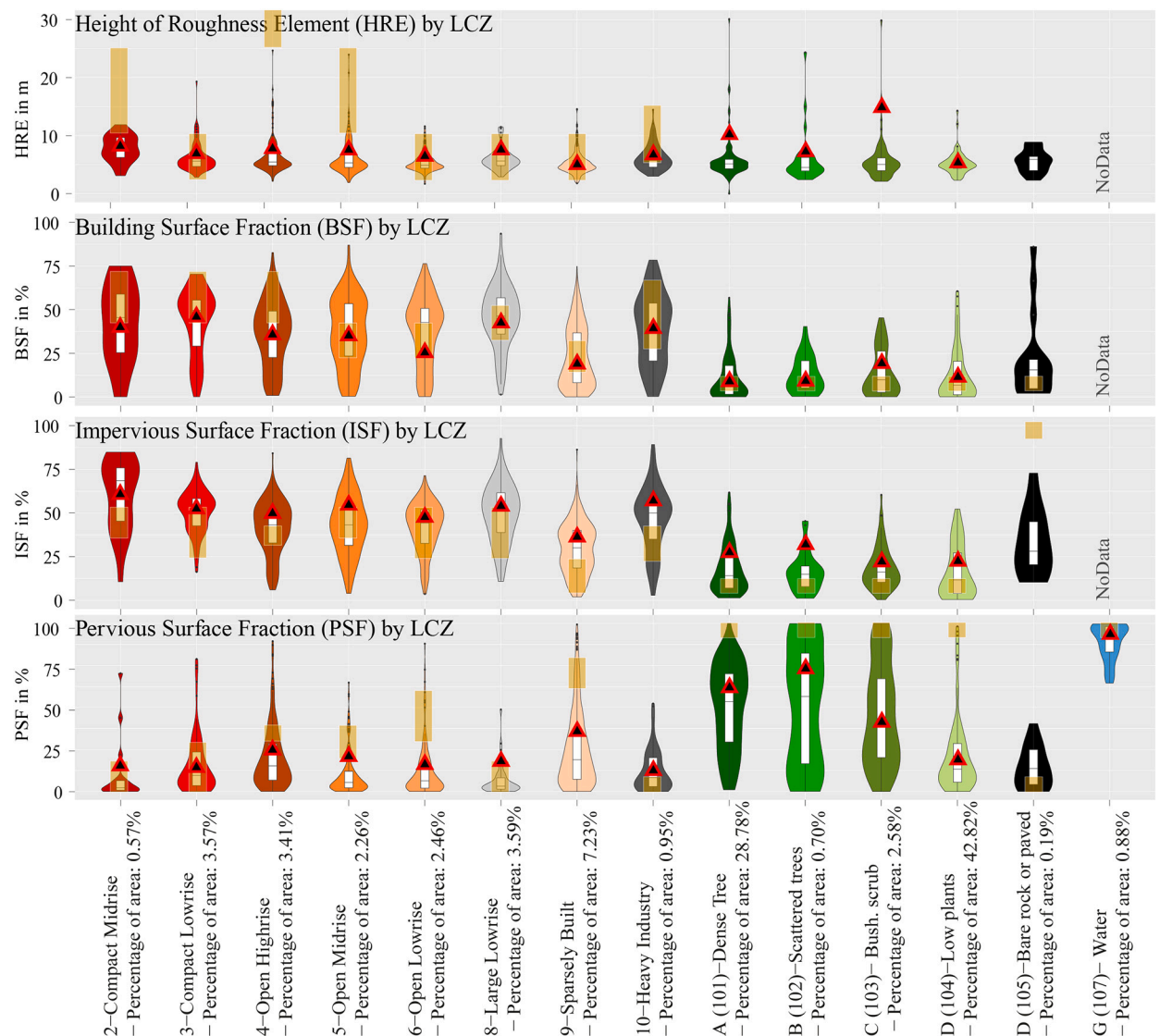


Fig. 6. Properties of each LCZ category in terms of Height of Roughness Element (HRE), Building Surface Fraction (BSF), Impervious Surface Fraction (ISF) and Pervious Surface Fraction (PSF). The violin plots and triangles show the LCZ properties for the whole of Dijon Métropole and for the VeloClim transect, respectively. The rectangles in yellow show the LCZ properties as defined by Stewart and Oke (2012). (For interpretation of the references to colour in this figure legend, the reader is referred to the web version of this article.)

To validate the LCZs obtained in Dijon Métropole, Fig. 6 compares their properties to canonical LCZs using four metrics defined by Stewart and Oke (2012) and Geletič and Lehnert (2016): the Height of Roughness Element (HRE), the Building Surface Fraction (BSF), the Impervious Surface Fraction (ISF) and the Pervious Surface Fraction (PSF). These metrics have been computed for both the whole city and along the transect (violin plots and triangles in Fig. 6, respectively) using the BD TOPO database (IGN, 2016; Emery et al., 2017) describing urban morphology across France. The accuracy of our classification depends on the metric considered. Compared to canonical LCZs (Stewart and Oke, 2012), HRE is underestimated by 52% over densely built categories (LCZs 2, 4 and 5) because of a local political decision to limit the height of buildings. PSF also tends to be underestimated, especially for LCZs with vegetation (LCZs A, B, C and D). This bias reaches ~50%. It is mainly the consequence of shortcomings with the BD TOPO database in describing low vegetation and even overall vegetation when its coverage is less than 200 m². Hence, the PSF is underestimated by ~90% for LCZ D. On the other hand, the BSF and, to a larger extent, ISF, accurately fit the canonical values provided by Stewart and Oke (2012), lending credibility to our classification. It is also worth noting that the LCZ properties are generally closer to the canonical values when computed along the transect than for the Dijon metropolitan area as a whole.

3.2. Impact of CLCs/LCZs on temperature along the transect

To properly assess the impact of urban form on air temperature, Stewart and Oke (2012) recommend avoiding the mixed influence of different LCZs and, by extension, CLCs on air temperature. To do so, we consider a buffer of 400 m around each record and keep only

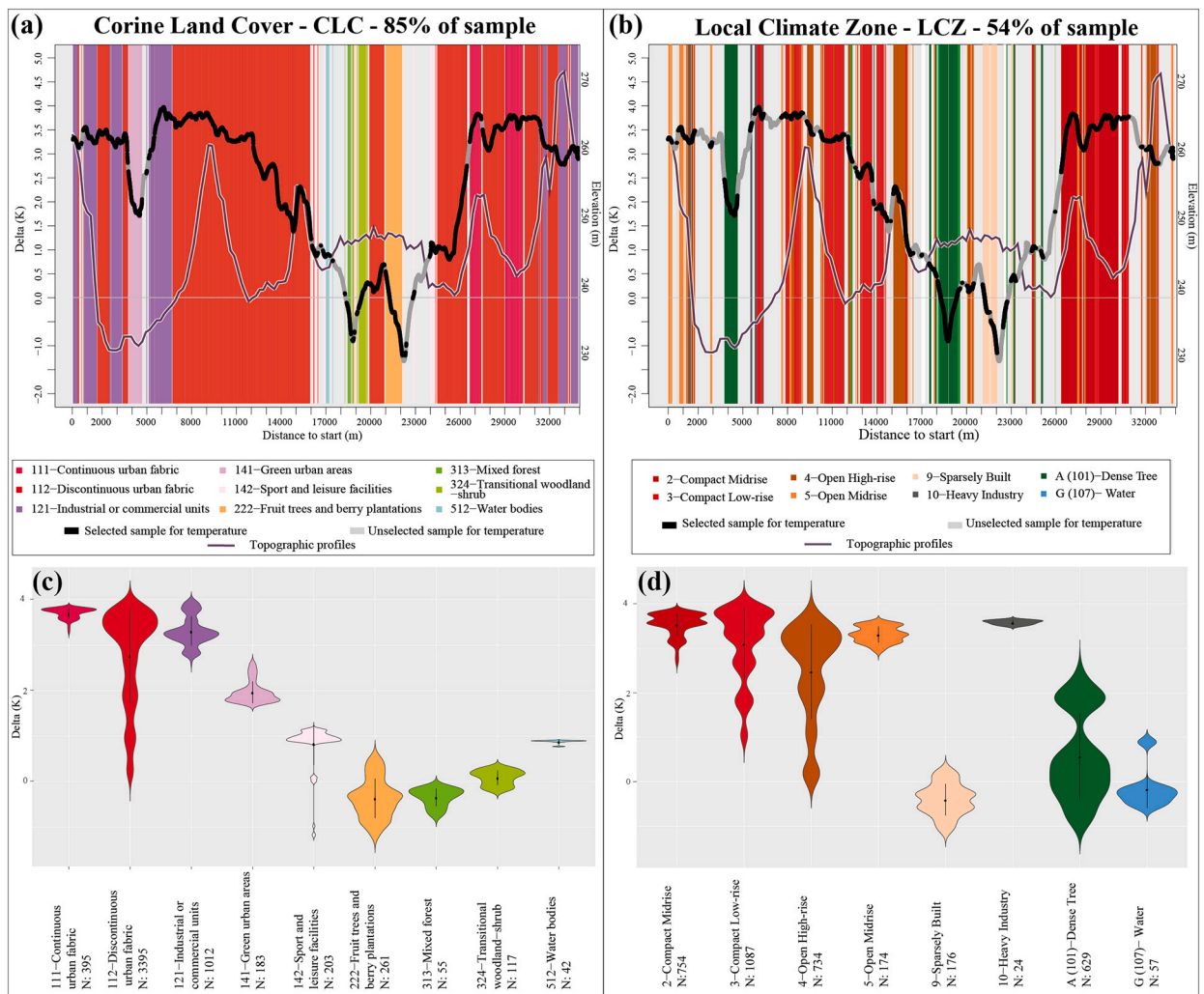


Fig. 7. Temperature and urban form along the transect. (a) Temperature differences against the rural index, averaged for the 24 runs (black and white line) together with the CLC categories (shadings) and the altitude (grey line). The influence of urban form on temperature is assessed when at least 55% of the area in a 400 m radius around each temperature record is covered by the same CLC (see section 3.2). The selected sample is shown in black for temperature and in shades of colour for CLC categories. (b) Same as (a) but for LCZ categories. (c) Temperature differences for the 24 runs associated with each CLC category. (d) Same as (c) but for each LCZ category.

those records when at least 55% of the buffer area is covered by a single LCZ or CLC category. This criterion guarantees the selection of temperature in homogeneous urban categories without reducing the sample size too drastically. The different buffer sizes tested (i.e. 400 m and 1000 m) lead to similar results (not shown). The sample selected for analysing the urban form–temperature relationship in the remainder of this study is shown in black in Fig. 4. It corresponds to 85% of temperature records for CLCs and 54% for LCZs. About 85% (15%) of this sample belong to urban (natural) environments for CLCs, differing slightly from the proportions for LCZs (~80% versus 20%).

3.2.1. Impact on mean temperature

The mean temperature differences averaged over the 24 runs (see section 3.1 for details on their computation) are shown along the transect in Fig. 7 together with the altitude and all corresponding CLC/LCZ categories. On average, temperature differences vary between -1.5 K and + 4 K along the transect (against the rural index derived from the MUSTARDijon network: see section 2.3), hence a marked spatial amplitude of 5.5 K (Fig. 7a. and 7b). Altitude changes partially explain temperature variability along the transect, as reflected by the thermal inversion of ~1 K between the plain (km 1 to 16 and 26 to 33 in Fig. 7a and b) and the valley (km 16 to 25). The impact of altitude on temperature remains weak, though, (spatial correlation close to 0) and cannot account, for example, for the abrupt variation in temperature between km 17 and 24. On the other hand, the urban form categories seem to play a major role

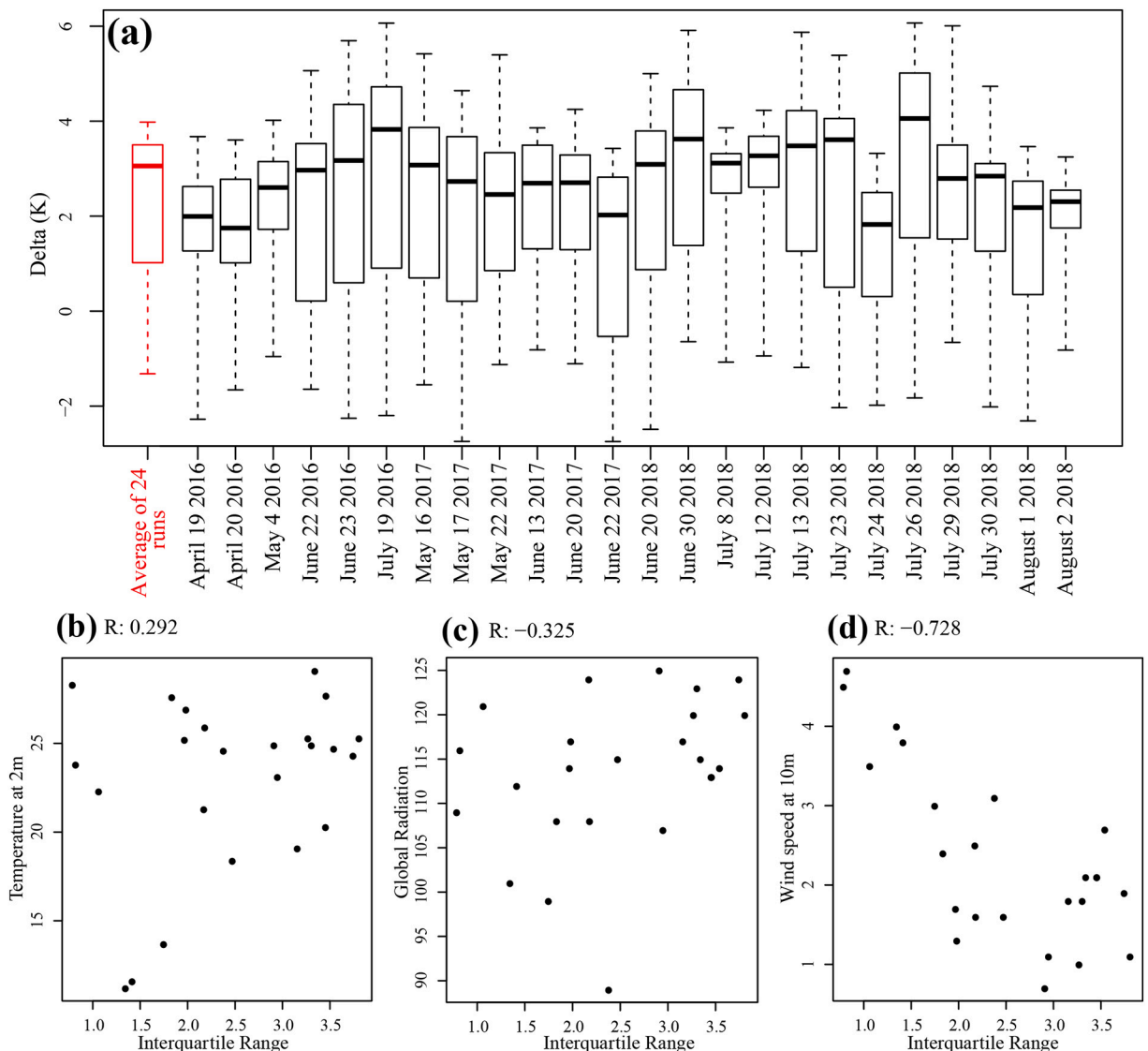


Fig. 8. Spatial variability of temperature along the transect and relationship with weather conditions. (a) Spatial variability of temperature for each run and averaged for the 24 runs. (b) Relationship between temperature spatial variability defined as the interquartile range (x-axis; rectangle in panel a) and 2 m temperature recorded at Dijon-Longvic and averaged between 19 and 21 UTC of each run (y-axis). (c) Same as (b) but for global radiation averaged between 06 and 18 UTC. (d) Same as (c) but for wind speed at 10 m averaged between 19 and 21 UTC.

regardless of the typology considered. Areas with the highest temperatures correspond to categories describing highly artificial, mineral, and impervious surfaces (e.g. CLCs 111, 112 and 121 in Fig. 7a; LCZs 2, 3, 4, 5 and 10 in Fig. 7b). By contrast, the coolest areas correspond to sparsely built and, to a larger extent, highly vegetated zones (CLCs 222, 313, 324 and 512; LCZs 9, A and G).

These qualitative results are confirmed by ANOVAs computed using the temperature averaged over the 24 runs, and indicating that ~60% (~70%) of the temperature variability along the transect is explained by the 9 CLCs (8 LCZs) (see Fig. 9). This is further confirmed by the distribution of temperature differences of the 24 runs according to the CLCs/LCZs (Fig. 7c-d, respectively). The temperature distribution also indicates that the influence of urban form on air temperature is by no means perfect. For instance, temperature variability remains non-negligible within CLC 112 and LCZs 3 and 4, which lie at the intersection between densely built and highly vegetated zones (Fig. 4). This is also the case for LCZ A, which depicts a bi-modal distribution of temperature differences against the rural index. LCZ A corresponds mainly to (1) the 33 ha urban park located south of the city centre and (2) forests/gardens located in the western part of the city. These two zones, although similarly characterized by local minima of temperature (Fig. 7b), nonetheless display very dissimilar temperature levels (the urban park area being warmer). This is probably due to (1) the proximity between the city centre and the park and (2) the slight thermal inversion discussed above and that cools the gardens located in the lower parts of the valley, west of the conurbation.

3.2.2. Impact on temporal variability

The above analysis provides an average view of the impact of CLC and LCZ categories on temperature, which may overestimate the relative weight of surface conditions by increasing the signal (static surface properties, including urban form and soil sealing) to noise (atmospheric dynamics, including synoptic wind and atmospheric turbulence) ratio. Here, we go one step further by assessing (1) the spatial variability of temperature along the transect for the 24 runs, (2) the role of weather conditions in modulating that variability and (3) the consequences for the urban form–temperature relationship for both typologies.

Fig. 8a shows the spatial variability of temperature for each of the 24 runs. All the runs are markedly different from the mean run shown in red and considered so far. The median of the temperature difference with surrounding rural stations ranges from +2 K to +4 K. This confirms that all runs were conducted in the presence of UHIs. Two main types of UHIs emerge: those associated with high spatial variability in temperature along the transect (11 out of the 24 runs: 22 and 23 June 2016, 19 July 2016, 16 and 17 May 2017, 22 June 2018, 20 and 30 June 2018, 13, 23 and 26 July 2018) and those associated with low variability (the 13 remaining runs). Fig. 8b-d intersects the spatial variability of temperature along the transect, as measured by the interquartile range, with three hourly parameters recorded at the Météo-France synoptic weather station (see Fig. 1a) during each run: temperature and wind speed, both averaged between 19 and 21 UTC, and global radiation averaged between 06 and 18 UTC (that is, the day before the runs). Temperature spatial variability does not seem to be influenced by the background temperature conditions (Fig. 8b) nor by global radiation (Fig. 8c) for the 24 runs.

Wind has a marked impact, promoting more ventilation within the urban canopy layer, and so more homogeneous temperatures as its speed increases (Fig. 8d). The effect of wind speed on the urban form–temperature relationship is further assessed by intersecting the temperature variability within (x-axis) and between (y-axis) the CLC/LCZ categories for each run (Fig. 9a). Wind speed does not modulate the impact of CLC categories on temperature, since temperature variability between and within CLCs co-vary linearly (Fig. 9a, grey dots). However, the impact of LCZs on temperature tends to increase as wind speed decreases (and temperature spatial variability increases), as reflected by the exponential shape of the scatterplot (Fig. 9a, orange dots).

Importantly, the urban form explains more than 50% of the temperature variability along the transect in 21/23 out of the 24 runs for CLC/LCZ typologies, respectively (Fig. 9b). Except for a few runs (e.g. 29 and 30 July 2018), this contribution is almost

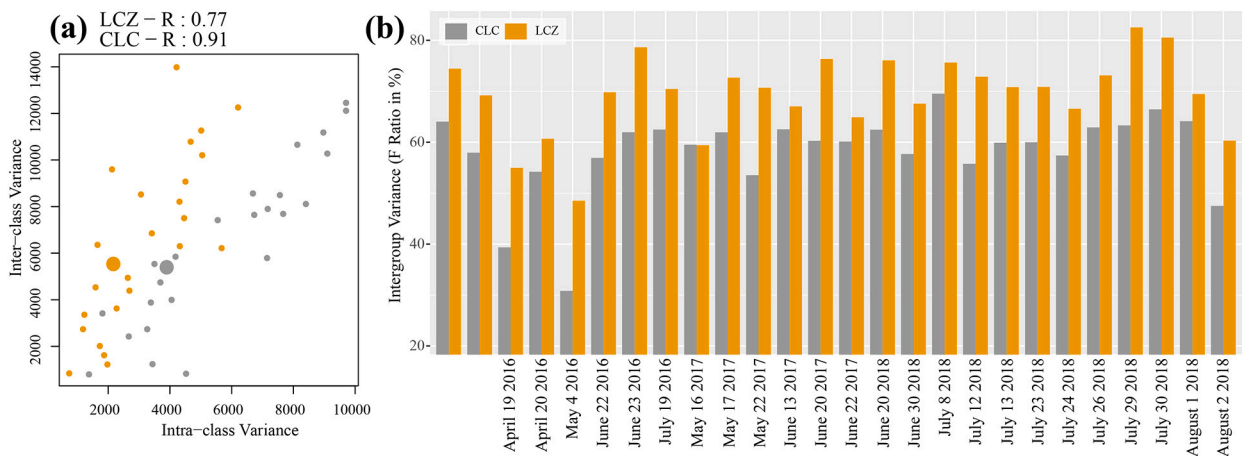


Fig. 9. Synthesis of ANOVA for each run. (a) Relation between intra-class and inter-class temperature variance for CLCs (grey) and LCZs (orange). Small/large dots represent each run/the 24-run mean. (b) Fraction of temperature variability (%) explained by each typology (CLC in grey and LCZ in orange).

systematically larger when temperature variability is high and wind speed is low. Therefore, the urban form remains the main driver of temperature spatial variability during occurrences of UHIs, and its impact is much greater under low wind speed conditions.

3.3. Effects of the different CLC and LCZ categories on air temperature

Previous sections indicate a strong and significant impact of the urban form on urban air temperature spatial variability. Here, we seek to identify the urban form categories that have the greatest impact on temperature, not only in terms of temperature differences, but also in terms of frequency. In other words, we attempt here to determine whether the influence of a given category is recurrent or occasional. For each of the 24 runs, we compare temperature differences of the different categories in each typology against CLC 111 and LCZ 2 using the Tukey test (see section 2.4). Fig. 10 summarizes the results for the 24 runs and Table 1 shows the number of runs (as a percentage) when temperatures associated with each category differ significantly (either warmer or colder) from those of CLC 111/LCZ 2 at different confidence levels.

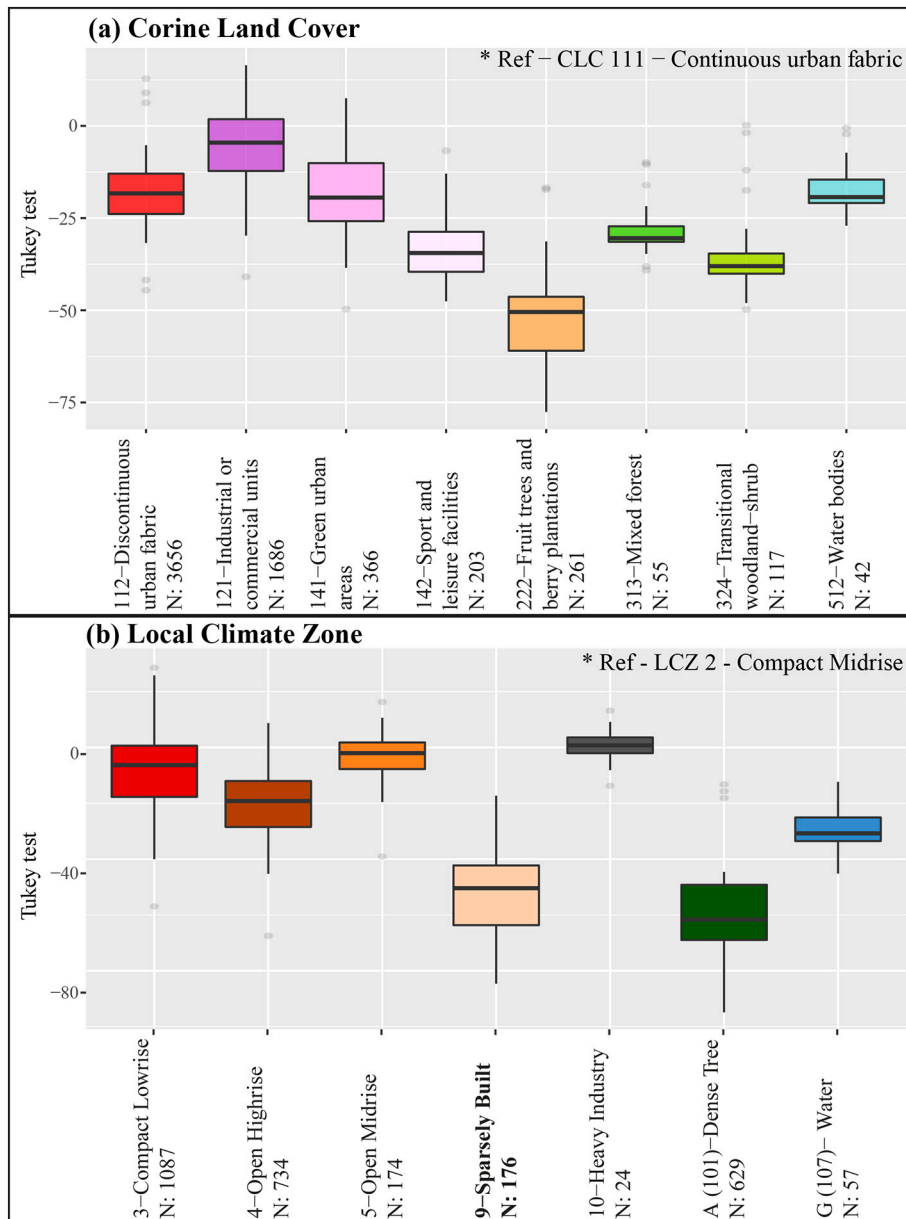


Fig. 10. Impact of each CLC and LCZ category on temperature for the 24 runs. (a) Result of the Tukey test between each CLC category and CLC 111 (continuous urban fabric). The more Tukey test values deviate from 0, the more the temperature associated with each CLC category differs from that of CLC 111. (b) Same as (a) but for LCZ categories compared to LCZ 2 (compact midrise).

Table 1

Percentage of runs when temperatures associated with a category are significantly different from those of the city centre (CLC 111 or LCZ 2). (a) CLC categories. (b) LCZ categories. The percentage is shown at the (***) 99.99%, (**) 99%, (*) 90% and (.) 95% confidence level according to the Tukey test.

Sign (a)	112-Discontinuous urban fabric - N: 3656	121-Industrial or commercial units - N: 1686	141-Green urban areas - N: 366	142-Sport and leisure facilities - N: 203	222-Fruit trees and berry plantations - N: 261	313-Mixed forest - N: 55	324-Transitional woodland-shrub - N: 117	512-Water bodies - N: 42
.	100%	80%	96%	100%	100%	100%	100%	92%
*	100%	80%	96%	100%	100%	100%	100%	92%
**	100%	72%	96%	100%	100%	100%	100%	92%
***	8%	0%	4%	20%	88%	0%	24%	0%
Signif. codes: 0 '***' 0,001 '**' 0,01 '*' 0,05 '.' - p-value: < 2,2e-16								
Sign (b)	3-Compact Low-rise - N: 1087	4-Open High-rise - N: 734	5-Open Midrise - N: 174	9-Sparsely Built - N: 176	10-Heavy Industry - N: 24	A (101)-Dense Tree - N: 629	G (107)- Water - N: 57	
.	88%	100%	76%	100%	72%	100%	100%	
*	88%	96%	72%	100%	60%	100%	100%	
**	88%	96%	72%	100%	52%	100%	100%	
***	4%	8%	0%	72%	0%	88%	8%	

Signif. codes: 0 '***' 0,001 '**' 0,01 '*' 0,05 '.' - p-value: < 2,2e-16

Both typologies point to two main groups acting differently on temperatures. The first group corresponds to built or impervious surfaces located from the city centre towards the outskirts (CLCs 112, 121 and 141; LCZs 3, 4, 5 and 10). Associated temperatures are mostly slightly cooler than the reference category. The second group describes peri-urban and natural environments (CLCs 142, 222, 313, 324 and, to a lesser extent, 512; LCZs 9, A and G), which are clearly cooler than the reference category. These two groups depict the contrast between impervious surfaces associated with warm temperatures and pervious surfaces leading to significantly cooler air temperatures.

Except for CLC 121 and LCZ 10, Table 1 demonstrates that temperatures associated with each category shown in Fig. 10 differ significantly from those of the reference category for at least 90% of the runs at the 90% confidence level. Among them, sparsely built zones (LCZ 9) and forests (CLC 222 and LCZ A) are characterized by the coolest temperatures, a signal significant at the 99.99% confidence level in at least 70% of the runs. This shows that the influence of vegetation is recurrent to some extent, and could be considered as quasi-systematic, during the nights conducive to the development of UHIs.

4. Discussion

This paper is an attempt to assess the impact of urban form on the spatial variability of temperatures on the local to micro scales based on mobile temperature measurements and two urban form typologies (CLC and LCZ). Such a quantification is a challenging exercise for four main reasons:

- First, mobile measurements are subject to lag errors (here, the response time of the temperature sensor is ~ 30 s at $5 \text{ m}\cdot\text{s}^{-1}$). Lag errors make it difficult to measure the “unadulterated” influence of the CLC/LCZ categories on temperature;
- Second, the relationship is sensitive to sample size. Here, the sample is much smaller for LCZs (54% of the temperature records) than for CLCs (85%). By construction, we introduce more heterogeneity in CLCs than LCZs. The same analysis conducted using the same sample (54%) leads to very similar results, with $\sim 70\%$ of the temperature variability explained by surface states regardless of the typology. This illustrates that the way temperatures are sampled within and between urban categories is critical to the quantification of their influence on temperatures;
- Third, the relationship between temperature and the CLC/LCZ categories is quantified through simple statistics (ANOVA). This approach does not account for warm/cold advection from one CLC/LCZ category to the surrounding ones. For instance, LCZ A (dense trees) mixes a 33 ha urban park close to the city centre and forests located in the western part of the city that both have the effect of lowering temperatures but with different amplitudes because the influence of adjacent LCZ categories is not explicitly considered. In this particular case, temperatures in the urban park may also be influenced by warmer temperatures recorded around the park. More sophisticated approaches or a physical based analysis (e.g. urban climate modelling) are required to account for temperature advection and interactions between the different CLC/LCZ categories;
- Last, other physical features (e.g. altitude) and atmospheric circulation also affect temperature variability and may exacerbate or counter-balance the influence of urban form. The cases studied here correspond to calm weather conditions conducive to UHI development. The temperature along the transect is not correlated to the altitude profile (Fig. 7a-b), suggesting a weak control of altitude on temperature during the campaign. While wind speed remains relatively low during all runs, the influence of CLC/LCZ categories clearly decreases for the most windy runs ($3\text{--}4 \text{ m}\cdot\text{s}^{-1}$). Consistent with Brandsma and Wolters (2012) and Lehnert et al. (2018), low wind speeds result in less ventilation of the urban canopy layer and promote UHIs on the meso scale and spatially more heterogeneous temperatures on the local scale. In this study, we merely used wind speed from the synoptic weather station located south of the city (Fig. 1a), but the synoptic wind often differs markedly from the local wind conditions prevailing throughout the city. Here, the wind measurements made at 13 fixed locations along the VeloClim transect during all runs appear of little use for further interpreting temperature variability patterns, since the runs correspond to calm evenings and wind speeds were found to be within the instrumentation error range.

Despite the above limitations, two robust conclusions emerge from our study. Qualitatively, the CLC and LCZ typologies reveal a significant influence of urban form on temperature variability within the city, and between the city and its surrounding environment. Among the different CLC/LCZ categories, two major groups strongly impact temperatures. Densely built zones characterized by artificial, mineral and impervious surfaces are recurrently associated with warm temperatures and UHIs. By contrast, vegetated zones tend to cool temperatures and may promote UCIs. These effects are consistent with those identified in many cities worldwide over the last 100 years (Stewart, 2019). Quantitatively, our paper points to high sensitivity of the relationship between temperature and urban form on the local to micro scales depending on the typology used to synthesize surface properties. The CLC typology provides a macro-scale summary of surface properties and is thus less efficient for discriminating intra-urban temperature variability than the micro-scale summary provided by the LCZ typology (Fig. 9b). This is not surprising since the different CLC categories do not account for building characteristics (e.g. height and density), which are known to influence temperatures (Howard, 1833; Berg and Metzler, 1934; Oke, 2006; Stewart, 2019). Moreover, they can mix heterogeneous surfaces. For instance, CLC 112 merges small urban parks, housing estates, collective housing, detached housing and private gardens that may have antagonistic effects on temperatures. While our LCZ categories have some limitations induced by the WUDAPT approach (Lehnert, 2021) and the input data (BD TOPO), they better discriminate surface properties and are thus more suitable than CLCs when it comes to assessing urban form effects on urban climate (see e.g. Fig. 9b). The LCZ typology better discriminates surface properties and is thus more suitable than CLC for assessing urban form effects on urban climate (see e.g. Fig. 9b). This corroborates previous work (Buttstädt et al., 2011; Leconte et al., 2017; Lehnert et al., 2018).

5. Conclusion

This paper presents the results of a mobile measurement campaign involving repeated runs over the same transect in a medium-sized French conurbation. The results improve our understanding of the influence of surface conditions on air temperature at 2 m above ground level on a local scale, as seen by two different and complementary typologies of urban form. Analysis of temperature spatial variability cross-validated with CLC and LCZ categories has made it possible to reveal a marked and significant effect of certain types of urban form and their properties on UHIs and UCIs, independently of the background temperature. According to the two typologies tested, the urban developments that promote less intense UHIs have two major characteristics: (1) a low density of building (but not necessarily of population as in the case of LCZ 9) and (2) the presence of mixed high and low vegetation. Several major points about the effects in urban settings are noticeable:

- CLC and LCZ typologies are relevant and complementary for analysing the heterogeneity of surface contrasts on the scale of the urban space.
- On a local scale, the urban form has a decisive effect on air temperature independently of weather conditions. Temperature variability appears to be driven essentially by surface conditions (especially urban morphology and soil sealing). However, this claim should be nuanced by noting that, for this measurement campaign, weather conditions were similar with little wind and few clouds during the daytime, thereby maximizing the influence of surface properties on local air temperature.
- Accordingly, urban form has a greater effect on air temperature when spatial temperature constraints are strong and wind speed is low. Under windy conditions, temperatures become more uniform across the city, the weather takes the upper hand and the temperature pattern reflects spatial structures of a larger scale, thereby reducing the influence of surface conditions.
- The evenings when the surface contribution is weakest are the same for both typologies (CLC and LCZ), suggesting that the large-scale weather patterns, especially wind speed, prevail over surface conditions at those times.
- The LCZ typology is suitable for discriminating and understanding temperatures on a local scale, whereas CLC cannot readily account for the diversity of intra-urban categories on a local scale. This is especially true for discontinuous urban zones.

The discriminating effect of CLC and LCZ categories on air temperature can be explained primarily by their intrinsic characteristics, such as the impervious surfaces, the shape and size of the built area, the occurrence and type of vegetation. The most heavily vegetated surfaces, with both grass and trees, and surfaces associated with the presence of water, very likely promote night time urban cooling and may lead to the formation of UCIs. Even so, these zones are not widespread and vary in size. Developments such as allotments, and not just large zones of vegetation, may play a part in improving thermal comfort on summer evenings and nights. Less dense, more scattered buildings and the presence of a vegetation zone in residential areas are developments that are generally cooler than the city centre, conducive to UCIs within urban environments. The results achieved in this work suggest therefore that vegetation in cities is a primordial condition and recurrently effective over time for cooling urban air on evenings following sunny days with little wind. Vegetation in the city therefore seems to be a type of land cover and surface state that can significantly attenuate UHI phenomena and so help cities adapt to climate change while providing ecosystem and landscape services.

Declaration of competing interest

All of the authors declare that they have no known competing financial interests or personal relationships that could have appeared to influence the work reported in this paper.

Acknowledgements

The authors thank the anonymous reviewers for their constructive comments. The authors are grateful to all the volunteer cyclists who made this study possible: 13 in all who gave their pedal power to cover the 33.9 km of the route for a total 1155 km for the measurement campaign. In addition to most of the authors, these were Benjamin Bois, Etienne Brulebois, Xavier Hébert, Michel Perrin, Alexandre Pohl, Arnaud Rocha, and Pascal Roucou. This work is a contribution to the RESPONSE program (ERC H2020 Grant #957751: <https://h2020response.eu/>). The authors thank the Agence De l'Environnement et de la Maîtrise de l'Energie (ADEME) Bourgogne Franche-Comté, Dijon Métropole, Météo-France, and the Centre de Calcul de l'Université de Bourgogne (CCuB) for their financial and technical support.

References

- Bechtel, B., Daneke, C., 2012. Classification of local climate zones based on multiple earth observation data. *Sel. Top. Appl. Earth Obs. Remote Sens. IEEE J. Of 5*, 1191–1202. <https://doi.org/10.1109/JSTARS.2012.2189873>.
- Bechtel, B., Alexander, P.J., Beck, C., Böhner, J., Brousse, O., Ching, J., Demuzere, M., Fonte, C., Gál, T., Hidalgo, J., Hoffmann, P., Middel, A., Mills, G., Ren, C., See, L., Sismanidis, P., Verdonck, M.-L., Xu, G., Xu, Y., 2019. Generating WUDAPT level 0 data – current status of production and evaluation. *Urban Clim.* 27, 24–45. Doi:10/gf3x3w.
- Beck, C., Straub, A., Breitner, S., Cyrus, J., Philipp, A., Rathmann, J., Schneider, A., Wolf, K., Jacobeit, J., 2018. Air temperature characteristics of local climate zones in the Augsburg urban area (Bavaria, southern Germany) under varying synoptic conditions. *Urban Clim.* 25, 152–166. <https://doi.org/10.1016/j.uclim.2018.04.007>.
- Berg, H., Metzler, H.K., 1934. Temperaturemessfahrten durch das Gebiet der Stadt Hannover [temperature measurements on journeys through the neighbourhood of Hannover]. *Meteorologische Zeitschrift, Bioklimatische Beiblätter* 1, 111–114.

- Brandsma, T., Wolters, D., 2012. Measurement and statistical modeling of the urban Heat Island of the City of Utrecht (the Netherlands). *J. Appl. Meteorol. Climatol.* 51, 1046–1060. <https://doi.org/10.1175/JAMC-D-11-0206.1>.
- Brooks, C.F., 1931. How may one define and study local climates? *Comptes Rendus du Congrès International de Géographie 2. Paris.* 291–300.
- Brousse, O., Martilli, A., Foley, M., Mills, G., Bechtel, B., 2016. WUDAPT, an efficient land use producing data tool for mesoscale models? Integration of urban LCZ in WRF over Madrid. *Urban Clim.* 17, 116–134. <https://doi.org/10.1016/j.uclim.2016.04.001>.
- Büttner, G., Feranec, J., Jaffrain, G., 2002. Corine land cover update 2000 - Technical guidelines [I&CLC2000 project] (No. 89). European Environment Agency, Copenhagen.
- Budel, A., Wolf, J., 1933. Münchener stadtklimatische Studien [Munich town climatic studies]. *Zeitschrift für angewandte Meteorologie* 49, 4–10.
- Buttstädt, M., Sachsen, T., Ketzler, G., Merbitz, H., Schneider, C., 2011. A new approach for highly resolved air temperature measurements in urban areas. *Atmospheric Meas. Tech. Discuss.* 4, 1001–1019. <https://doi.org/10.5194/amtd-4-1001-2011>.
- Ching, J., Mills, G., Bechtel, B., See, L., Feddema, J., Wang, X., Ren, C., Brousse, O., Martilli, A., Neophytou, M., Mouzourides, P., Stewart, I., Hanna, A., Ng, E., Foley, M., Alexander, P., Aliaga, D., Niyogi, D., Shreevastava, A., Bhalachandran, P., Masson, V., Hidalgo, J., Fung, J., Andrade, M., Baklanov, A., Dai, W., Milcinski, G., Demuzere, M., Brunzell, N., Pesaresi, M., Miao, S., Mu, Q., Chen, F., Theeuwes, N., 2018. WUDAPT: an urban weather, climate, and environmental modeling infrastructure for the Anthropocene. *Bull. Am. Meteorol. Soc.* 99, 1907–1924. <https://doi.org/10.1175/BAMS-D-16-0236.1>.
- Eliasson, I., 1996. Urban nocturnal temperatures, street geometry and land use. In: *Atmos. Environ., Conference on the Urban Thermal Environment Studies in Tohwa*, 30, pp. 379–392. [https://doi.org/10.1016/1352-2310\(95\)00033-X](https://doi.org/10.1016/1352-2310(95)00033-X).
- Emery, J., Dudek, J., Granjon, L., Pohl, B., Richard, Y., Thévenin, T., Martiny, N., 2017. Chapter 3: characterizing urban morphology for urban climate simulation based on a GIS approach. In: *Teledetection et SIG. Toulouse, France.*
- Fenner, D., Meier, F., Scherer, D., Polze, A., 2014. Spatial and temporal air temperature variability in Berlin, Germany, during the years 2001–2010. In: *Urban Clim., ICUC8: The 8th International Conference on Urban Climate and the 10th Symposium on the Urban Environment 10*, pp. 308–331. <https://doi.org/10.1016/j.uclim.2014.02.004>.
- Fouillet, A., Rey, G., Laurent, F., Pavillon, G., Bellec, S., Guihenec-Jouyau, C., Clavel, J., Jougla, E., Hémon, D., 2006. Excess mortality related to the august 2003 heat wave in France. *Int. Arch. Occup. Environ. Health* 80, 16–24. <https://doi.org/10.1007/s00420-006-0089-4>.
- Fukui, E., Wada, T., 1941. Horizontal distribution of air temperature in the great cities of Japan. In *Japanese Geogr. Rev.* Jpn 17, 354–372.
- Gál, T., Bechtel, B., Unger, J., 2015. Comparison of two different local climate zone mapping methods. In: *ICUC9 - 9th International Conference on Urban Climate Jointly with 12th Symposium on the Urban Environment*. Presented at the ICUC9 - 9th International Conference on Urban Climate Jointly with 12th Symposium on the Urban Environment, Toulouse, France.
- Geletić, J., Lehnert, M., 2016. GIS-based delineation of local climate zones: the case of medium-sized central European cities. *Morav. Geogr. Rep.* 24, 2–12. <https://doi.org/10.1515/mgr-2016-0012>.
- Giffinger, R., Fertner, C., Kramar, H., Meijers, E., 2007. City-ranking of European medium-sized cities. *Cent Reg Sci* 1–12.
- Giffinger, R., Haindlmaier, G., Kramar, H., 2010. The role of rankings in growing city competition. *Urban Res. Pract.* 3, 299–312. <https://doi.org/10.1080/17535069.2010.524420>.
- Hajat, S., O'Connor, M., Kosatsky, T., 2010. Health effects of hot weather: from awareness of risk factors to effective health protection. *Lancet Lond. Engl.* 375, 856–863. [https://doi.org/10.1016/S0140-6736\(09\)61711-6](https://doi.org/10.1016/S0140-6736(09)61711-6).
- Hann, J., 1885. Über den Temperaturunterschied zwischen Stadt und land [on the temperature difference between town and country]. *Österreichischen Gesellschaft für Meteorologie, Zeitschrift* 20, 457–462.
- Hart, M.A., Sailor, D.J., 2009. Quantifying the influence of land-use and surface characteristics on spatial variability in the urban heat island. *Theor. Appl. Climatol.* 95, 397–406. <https://doi.org/10.1007/s00704-008-0017-5>.
- Haynes, W., 2013. Tukey's test. In: *Dubitzky, W., Wolkenhauer, O., Cho, K.-H., Yokota, H. (Eds.), Encyclopedia of Systems Biology*. Springer, New York, NY, pp. 2303–2304. https://doi.org/10.1007/978-1-4419-9863-7_1212.
- Heusinkveld, B.G., Steeneveld, G.J., van Hove, L.W.A., Jacobs, C.M.J., Holtslag, A.A.M., 2014. Spatial variability of the Rotterdam urban heat island as influenced by urban land use. *J. Geophys. Res.-Atmos.* 119, 677–692. <https://doi.org/10.1002/2012JD019399>.
- Howard, L., 1833. *The Climate of London Deduced from Meteorological Observations, Made in the Metropolis, and at Various Places Around It, vols. 1–3.* Harvey and Darton, London.
- IGN, 2016. *Descriptif de la BD TOPO Descriptif de contenu No. Révision du document de 2011.* Saint Mandé.
- Joly, D., Brossard, T., Cardot, H., Cavailhes, J., Hilal, M., Wavresky, P., 2010. Les types de climats en France, une construction spatiale. *Cybergeo Eur. J. Geogr.* <https://doi.org/10.4000/cybergeo.23155>.
- Kottek, M., Grieser, J., Beck, C., Rudolf, B., Rubel, F., 2006. World map of the Köppen-Geiger climate classification updated. *Meteorol. Z.* 259–263 <https://doi.org/10.1127/0941-2948/2006/0130>.
- Kropf, K., 2009. Aspects of urban form. *Urban Morphol.* 13, 105–120.
- Kropf, Karl, 2014. Ambiguity in the definition of built form. *Urban Morphol.* 18 (1), 41–57.
- Leconte, F., Bouyer, J., Claverie, R., Pétrissans, M., 2015. Using local climate zone scheme for UHI assessment: evaluation of the method using mobile measurements. *Build. Environ.* 83, 39–49. <https://doi.org/10.1016/j.buildenv.2014.05.005>. Special Issue: Climate adaptation in cities.
- Leconte, F., Bouyer, J., Claverie, R., Pétrissans, M., 2017. Analysis of nocturnal air temperature in districts using mobile measurements and a cooling indicator. *Theor. Appl. Climatol.* 130, 365–376. <https://doi.org/10.1007/s00704-016-1886-7>.
- Lehnert, M., Geletić, J., Dobrovolný, P., Jurek, M., 2018. Temperature differences among local climate zones established by mobile measurements in two central European cities. *Clim. Res.* 75, 53–64. <https://doi.org/10.3354/cr01508>.
- Lehnert, M., Savić, S., Milošević, D., Dunjić, J., Geletić, J., 2021. Mapping local climate zones and their applications in European urban environments: a systematic literature review and future development trends. *ISPRS Int. J. Geo-Inf.* 10, 260. <https://doi.org/10.3390/ijgi10040260>.
- Ng, E., Ren, C., Mills, G., Mochida, A., YUAN, C., Matzarakis, A., Mayer, H., Katzschner, L., Baumuller, J., Oke, T., Stewart, I., Thorsson, S., Lindberg, F., Chapman, L., Huang, B., Jusuf, S., Lau, K., Lindley, S., Moriyama, M., Cavan, G., 2015. The Urban Climatic Map: A Methodology for Sustainable Urban Planning.
- Oke, 1973. City size and the urban heat island. *Atmos. Environ.* 1967 (7), 769–779. [https://doi.org/10.1016/0004-6981\(73\)90140-6](https://doi.org/10.1016/0004-6981(73)90140-6).
- Oke, T.R., 1983. *WCP, 45. Bibliography of urban climate 1977–1980.* WMO, Geneva.
- Oke, 2006. Towards better scientific communication in urban climate. *Theor. Appl. Climatol.* 84, 179–190. <https://doi.org/10.1007/s00704-005-0153-0>.
- Pascal, M., Wagner, V., Corso, M., Laaidi, K., Ung, A., Beaudou, P., 2018. Heat and cold related-mortality in 18 French cities. *Environ. Int.* 121, 189–198. <https://doi.org/10.1016/j.envint.2018.08.049>.
- Peppler, A., 1929. Das auto als Hilfsmittel der meteorologischen Forschung [the auto as an aid to meteorological investigation]. *Zeitschrift für angewandte Meteorologie* 46, 305–308.
- Petralli, M., Massetti, L., Brandani, G., Orlandini, S., 2014. Urban planning indicators: useful tools to measure the effect of urbanization and vegetation on summer air temperatures. *Int. J. Climatol.* 34 <https://doi.org/10.1002/joc.3760>.
- Petrişor, A.-I., Petrişor, L.E., 2015. Assessing microscale environmental changes: CORINE Vs The Urban Atlas. *Present Environ. Sustain. Dev.* 9, 95–104. <https://doi.org/10.1515/pesd-2015-0027>.
- Rajkovich, N.B., Larsen, L., 2016. A bicycle-based field measurement system for the study of thermal exposure in Cuyahoga County, Ohio, USA. *Int. J. Environ. Res. Public Health* 13, 159. <https://doi.org/10.3390/ijerph13020159>.
- Renou, E., 1868. Différences de température entre la ville et la campagne [Temperature differences between town and country]. In: *Annuaire, Société Météorologique de France*, 16, pp. 83–97.
- Revi, A., Satterthwaite, D., Aragón-Durand, F., Corfee-Morlot, J., Kiunsi, R., Pelling, M., Roberts, D., Solecki, W., 2014. Urban areas in climate change 2014: impacts, adaptation, and vulnerability. Part a: global and Sectoral aspects. In: *Contribution of Working Group II to the Fifth Assessment Report of the Intergovernmental Panel on Climate Change.* Cambridge, United Kingdom and New York, pp. 535–612.

- Richard, Y., Emery, J., Dudek, J., Pergaud, J., Chateau-Schmith, C., Zito, S., Rega, M., Vairet, T., Castel, T., Thévenin, T., Pohl, B., 2018. How Relevant Are Local Climate Zones, Urban Climate Zones, and USGSDijon for Urban Climate Research? Dijon (France) as a Case Study (Urban Clim).
- Richard, Y., Pohl, B., Rega, M., Pergaud, J., Thevenin, T., Emery, J., Dudek, J., Vairet, T., Zito, S., Chateau-Smith, C., 2021. Is urban Heat Island intensity higher during hot spells and heat waves (Dijon, France, 2014–2019)? Urban Clim. 35, 100747. <https://doi.org/10.1016/j.uclim.2020.100747>.
- Robine, J.-M., Cheung, S.L.K., Le Roy, S., Van Oyen, H., Griffiths, C., Michel, J.-P., Herrmann, F.R., 2008. Death toll exceeded 70,000 in Europe during the summer of 2003. C. R. Biol. 331, 171–178. <https://doi.org/10.1016/j.crv.2007.12.001>.
- Runnalls, K., Oke, T., 2013. Dynamics and controls of the near-surface heat island of Vancouver British Columbia. Phys. Geogr. 21, 283–304. <https://doi.org/10.1080/02723646.2000.10642711>.
- Schmidt, W., 1927. Die Verteilung der Minimumtemperaturen in der Frostnacht des 12. Mai 1927 im Gemeindegebiete von Wien [Distribution of minimum temperatures during the frost night of May 12, 1927, within the communal limits of Vienna]. Fortschritte der Landwirtschaft 2, 681–686.
- Shapiro, S.S., Wilk, M.B., 1965. An analysis of variance test for normality (complete samples). Biometrika 52, 591–611. <https://doi.org/10.1093/biomet/52.3-4.591>.
- Song, J., Du, S., Feng, X., Guo, L., 2014. The relationships between landscape compositions and land surface temperature: quantifying their resolution sensitivity with spatial regression models. Landsc. Urban Plan. 123, 145–157. <https://doi.org/10.1016/j.landurbplan.2013.11.014>.
- Stewart, I.D., 2019. Why should urban heat island researchers study history? Urban Clim. 30, 100484. <https://doi.org/10.1016/j.uclim.2019.100484>.
- Stewart, I.D., Oke, T.R., 2012. Local climate zones for urban temperature studies. Bull. Am. Meteorol. Soc. 93, 1879–1900. <https://doi.org/10.1175/BAMS-D-11-00019.1>.
- Sun, C.-Y., 2011. A street thermal environment study in summer by the mobile transect technique. Theor. Appl. Climatol. 106, 433–442. <https://doi.org/10.1007/s00704-011-0444-6>.
- Sun, C.-Y., Brazel, A.J., Chow, W.T.L., Hedquist, B.C., Prashad, L., 2009. Desert heat island study in winter by mobile transect and remote sensing techniques. Theor. Appl. Climatol. 98, 323–335. <https://doi.org/10.1007/s00704-009-0120-2>.
- Sundborg, Å., 1951. Climatological studies in Uppsala with special regard to the temperature conditions in the urban area. In: Geographica. Geographical Institute of Uppsala, Sweden, p. 22.
- Takahashi, M., 1959. Relation between the air temperature distribution and the density of houses in small cities of Japan. In Japanese Geogr. Rev. Jpn 32, 305–313.
- Tan, J., Zheng, Y., Tang, X., Guo, C., Li, L., Song, G., Zhen, X., Yuan, D., Kalkstein, A.J., Li, F., 2010. The urban heat island and its impact on heat waves and human health in Shanghai. Int. J. Biometeorol. 54, 75–84. <https://doi.org/10.1007/s00484-009-0256-x>.
- Tsin, P.K., Knudby, A., Krayenhoff, E.S., Ho, H.C., Brauer, M., Henderson, S.B., 2016. Microscale mobile monitoring of urban air temperature. Urban Clim. 18, 58–72. <https://doi.org/10.1016/j.uclim.2016.10.001>.
- Tukey, J.W., 1962. The future of data analysis. Ann. Math. Stat. 33, 1–67. <https://doi.org/10.1214/aoms/1177704711>.
- Unger, J., Gál, T., Rakonczai, J., Mucsi, L., Szatmari, J., Tobak, Z., Van Leeuwen, B., Fiala, K., 2010. Modeling of the urban heat island pattern based on the relationship between surface and air temperatures. Időjárás 114, 287–302.
- Verdonck, M.-L., Okujeni, A., van der Linden, S., Demuzere, M., De Wulf, R., Vancoillie, F., 2017. Influence of neighbourhood information on ‘local climate zone’ mapping in heterogeneous cities. Int. J. Appl. Earth Obs. Geoinf. 62, 102–113. <https://doi.org/10.1016/j.jag.2017.05.017>.
- von Storch, H., Zwiers, F.W., 1999. Statistical Analysis in Climate Research. Cambridge University Press, Cambridge. <https://doi.org/10.1017/CBO9780511612336>.
- Zhou, B., Rybski, D., Kropp, J.P., 2013. On the statistics of urban heat island intensity. Geophys. Res. Lett. 40, 5486–5491. <https://doi.org/10.1002/2013GL057320>.